ELSEVIER

International Journal of Mass Spectrometry 214 (2002) 75–88

International Journal of Mass Spectrometry

www.elsevier.com/locate/ijms

Poly(propylene imine) dendrimer conformations in the gas phase: a tandem mass spectrometry study

Anuj Adhiya[1], Chrys Wesdemiotis*

Department of Chemistry, The University of Akron, Akron, OH 44325, USA

Received 29 August 2001; accepted 5 November 2001

Dedicated to Professor R. Graham Cooks on the occasion of his 60th birthday.

Abstract

$[M + H]^+$ ions are produced from a generation three poly(propylene imine) dendrimer (DAB-*dendr*-$(NH_2)_{16}$) by matrix-assisted laser desorption ionization (MALDI) or electrospray ionization (ESI), employing solvents of varying polarity and acidity for sample preparation (in MALDI) or the spraying process (in ESI). Subsequently, the structures of $[M + H]^+$ are investigated by tandem mass spectrometry (MS/MS), via the post-source decay (PSD) and collisionally activated dissociation (CAD) techniques. Upon MALDI-PSD, elimination of the outer branches, i.e., of $HN(CH_2CH_2CH_2NH_2)_2$ and $HN[CH_2CH_2CH_2N(CH_2CH_2CH_2NH_2)_2]_2$, is observed with a polar protic but not with a nonpolar solvent. Similarly, the loss of the outer branches upon ESI-CAD is discriminated against when employing a nonpolar instead of a polar protic solvent. These differences are attributed to the existence of distinct conformations for the neutral dendrimer and the $[M + H]^+$ ions formed from it. A nonpolar solvent leads to a folded conformation, i.e., one with the periphery branches pointing into the interior of the dendrimer to enable intramolecular hydrogen bonds. Due to such self-solvation, certain C–N bonds cannot be cleaved efficiently upon MS/MS. On the other hand, a polar protic solvent interacts favorably with the dendrimer through intermolecular hydrogen bonds, promoting the formation of an extended, unfolded conformation from which outer and periphery branches can readily be eliminated. These structural differences disappear in the $[M+2H]^{2+}$ cations produced by ESI; now, the loss of the outer branches takes place upon MS/MS irrespective of the solvent used in the ion generation step; this result is consistent with a stretched conformation for $[M+2H]^{2+}$, where the repulsion between the like charges is minimized. (Int J Mass Spectrom 214 (2002) 75–88) © 2002 Elsevier Science B.V. All rights reserved.

Keywords: Poly(propylene imine) dendrimer; Solvent effects; Dendrimer conformation; Folding; MALDI vs. ESI

1. Introduction

Dendrimers are a special class of highly symmetric three-dimensional macromolecules containing a core region, a repeating unit and a large number of peripheral groups. Their significant branching and surface functionality, combined with their low intrinsic viscosity, high miscibility/solubility and high reactivity, have led to useful applications in the areas of catalysis, recyclable solubilization, drug delivery and magnetic resonance imaging [1].

One of the most widely studied categories of dendrimers are poly(propylene imine) dendrimers composed of a 1,4-diaminobutane (DAB) core that is extended with propylene imine units (Scheme 1);

* Corresponding author. E-mail: wesdemiotis@uakron.edu

[1] Present address: Waters Corporation, 34 Maple St., Milford, MA 01757, USA.

1387-3806/02/$20.00 © 2002 Elsevier Science B.V. All rights reserved.
PII S1387-3806(01)00561-9

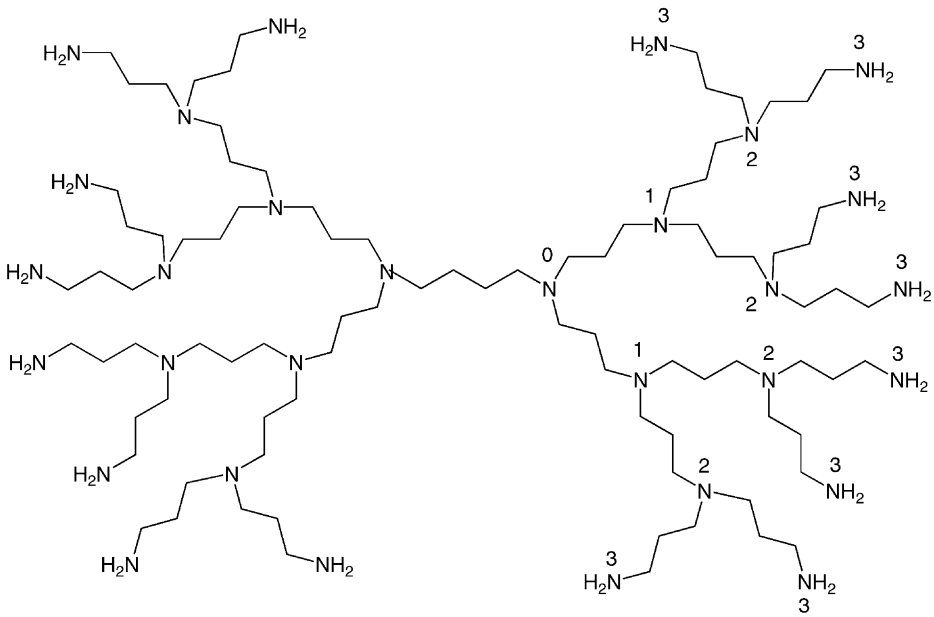

Scheme 1. Schematic representation of DAB-*dendr*-$(NH_2)_{16}$, a third generation dendrimer. The numbers next to the N atoms indicate the generation in which they are introduced. Only the right half is labeled.

these molecules have been termed DAB-*dendr*-$(NH_2)_x$, with x indicating the number of primary amine groups at the periphery [1]. The nitrogen atoms of the core are separated by four CH_2 groups, while three CH_2 groups separate all other N atoms from each other. Every successive layer of propylene imine units gives rise to a new generation dendrimer; hence, generations 1–4 have $x = 4$, 8, 16 and 64 peripheral NH_2. Scheme 1 illustrates a third generation DAB dendrimer, viz. DAB-*dendr*-$(NH_2)_{16}$ [1].

Dendrimers are prepared either in a convergent or divergent manner. In the convergent method, the dendritic wedges are produced separately and connected to a central core in the final step [2,3]. In the divergent synthesis, the dendrimer is grown in a sequential manner from a central core [4,5]. DAB dendrimers are usually synthesized via the divergent approach [1,4,5]. The first generation is obtained by Michael addition of DAB to acrylonitrile and subsequent hydrogenation of the nitrile groups. Repeating these reactions provides the second generation DAB dendrimer, etc. Statistical defects cannot be avoided in this procedure; e.g., only 68% of the third generation of a divergently produced dendrimer have a perfect (i.e. defect-free) structure [1].

Various NMR techniques (^1H, ^{13}C, ^{19}F, ^{31}P) [6–8], elemental analyses and chromatography [9,10] have been used to characterize DAB (and similar) dendrimers, but these techniques cannot disclose small amounts of impurities in, particularly, higher generation dendrimers. Mass spectrometry methods, on the other hand, especially electrospray ionization (ESI) [11] and matrix-assisted laser desorption ionization (MALDI) [12] mass spectrometry, have allowed the unequivocal identification of imperfections in DAB dendrimers. These were attributed to two possible side reactions, namely (1) incomplete cyanoethylation and retro-Michael reactions, resulting in missing propylene imine units, and (2) ammonia loss, leading to ring formation between two surface arms during nitrile hydrogenation [13,14].

There has been considerable interest in the conformations of DAB dendrimers and related polymers. In early studies, the monomers of each generation were assumed to be fully elongated and the end groups were

grouped in concentric circles around the core, suggesting that the dendrimer is a spherical body [15]. According to this model, dendrimers could grow freely and the core of the dendrimer had the lowest density. Later simulations showed that, after a certain point, the ends of the branches were not positioned at the surface but were severely back folded [16,17]. A self-consistent mean field model (SCMF) predicted flexible dendrimers to have dense, not hollow cores, with the ends distributed throughout the volume of the dendrimer [18]. Molecular dynamics calculations with two different force fields, representing a good and a bad solvent, revealed a definite degree of back folding in poly(propylene imine) dendrimers irrespective of the solvent; however, the back folding was more marked in the bad solvent [19a]. (A polymer swells and forms a large coil in a *good* solvent but shrinks and builds a dense globule in a *bad* or *poor* solvent [19b].) Other theoretical and experimental investigations have indicated that the hydrodynamic volumes of dendrimers appear to be temperature independent but strongly influenced by the choice of solvent; the dendrimers collapsed in poor solvents, while in good solvents a more open dendritic structure existed [20–22].

Poly(propylene imine) dendrimers with different end groups have been subjected to viscometry and small-angle neutron scattering (SANS) measurements [19,23]. The results indicated that such dendrimers are flexible, with a relatively homogeneous density distribution, which in turn presupposes that the end groups must be back folded to some degree. The SANS data on DAB dendrimers also showed that these molecules have a propensity to stretch when the amines are protonated, confirming the flexible nature of poly(propylene imine) dendrimers [23]. Very recent NMR studies unveiled that the conformation of DAB dendrimers varies depending on whether they are dissolved in polar protic (good) or nonpolar (poor) solvents [8]. In the polar protic solvent, the molecules had an extended conformation to maximize the hydrogen bonding interactions of the interior tertiary amines with the solvent's acidic protons. In the nonpolar solvent, NMR detected interactions between H atoms near the periphery and N atoms closer to the interior. This could be due to a folded conformation, in which the periphery branches fold into the interior of the molecule to enable intramolecular hydrogen bonding between the primary external and tertiary internal amine groups. Alternatively, the extra resonances in the nonpolar solvent could originate from intertwined chains of two dendrimers, in which intermolecular hydrogen bonding can take place. In the present study, the intrinsic conformations of singly and doubly protonated DAB dendrimers, formed from solutions in polar, polar protic or nonpolar media, are probed based on the fragmentation patterns of the dendrimer ions, as determined by tandem mass spectrometry (MS/MS) experiments [24].

ESI-MS/MS has successfully been used by Meijer and co-workers [25], Kistemaker and co-workers [26] and McLuckey et al. [27] to elucidate the dissociation pathways of protonated DAB dendrimers and the distribution of synthetic defects in such polymers. Meijer and co-workers postulated that the fragmentation of singly charged dendrimers proceeds via a chain of intramolecular S_N2 reactions [25]. It was argued that the diaminobutane nitrogen atoms are the most basic ones present (in the gas phase), and hence, protonation should mainly lead to $[M+H]^+$ ions carrying a protonated DAB core. As a consequence, the first nucleophilic displacement reaction should lead to a splitting of the dendrimer core, producing the starting material for a cascade of analogous nucleophilic displacements that create most of the observed MS/MS products. Meijer and co-workers rationalized the remaining major fragments by additional proton shifts and rearrangements [25].

Kistemaker and co-workers [26] and McLuckey et al. [27], on the other hand, suggested that the MS/MS spectra of $[M + H]^+$ from DAB dendrimers can be interpreted on the basis of S_N2 reactions involving attack from a neutral nitrogen that is either interior or exterior to the protonation site (interior is defined as closer to, or one of, the nitrogen atoms of the DAB core and exterior as more distant from the core). Protonation was assumed to occur at any of the tertiary nitrogens, thereby giving rise to a whole host of decomposition channels, which can explain all

major fragments. In contrast, the cascade fragmentation mechanism proposed by Meijer and co-workers [25] presumed exclusive protonation at one of the two core nitrogen atoms (vide supra). Notwithstanding this discrepancy, all previous MS/MS studies [25–27] concurrently concluded that the site(s) of protonation within the dendritic framework play(s) an important role in the fragmentation of $[M + H]^+$ and $[M + nH]^{n+}$. The position of the proton(s) depends on both the relative proton affinities of the N atoms and the Coulomb repulsion between neighboring protonated sites. With singly charged dendrimers, repulsive interactions are absent and fragmentation is directed by the relative proton affinities of the basic sites in the dendrimer. With multiply charged dendrimers, Coulomb repulsions prevail, leading principally to protonation of the peripheral tertiary amines and, hence, to distinct fragmentation patterns.

In the quoted MS/MS investigations, the DAB dendrimers were electrosprayed from polar protic solvents. In this article, we report MALDI- and ESI-MS/MS data of DAB-*dendr*-$(NH_2)_{16}$ that was dissolved in protic, polar or nonpolar solvents during the sample preparation (in MALDI) or spraying process (in ESI). Results obtained by post-source decay (PSD) [28] within a MALDI-time-of-flight (TOF) mass spectrometer and by collisionally activated dissociation (CAD) within an ESI ion trap mass spectrometer [29] were compared to assess whether the conformational differences detected by NMR in solution are preserved in the gas phase.

2. Experimental

The MALDI experiments were performed with a Bruker reflectron TOF mass spectrometer equipped with a nitrogen laser emitting at 337 nm (Reflex III, Bruker Daltonics, Billerica, MA). The ion source and reflector potentials were set at 20.0 and 22.5 kV, respectively. Solutions of the dendrimer (10 mg/mL) were prepared in four different solvents, viz. chloroform, acetonitrile–ethanol–water (50:45:5) mixture, methylene chloride and benzene. Dithranol, which was used as the matrix, was also dissolved in these solvents (10 mg/mL). Matrix and dendrimer solutions (both in the same solvent) were mixed in a 1:1 ratio, and ca. 0.5 μL of the final mixture were applied to the MALDI sample target. These conditions yielded abundant $[M + H]^+$ ions from DAB-*dendr*-$(NH_2)_{16}$. The mass scale was calibrated internally, using the calculated *m*/*z* values of $[M + H]^+$ (1686.727) and of the peak appearing 19 u ($NH_3 + H_2$) lower (1667.696).

The PSD spectra of $[M + H]^+$ from DAB-*dendr*-$(NH_2)_{16}$ were measured by tuning the preselector to transmit only this ion (complete isotopic cluster). The fragments from $[M + H]^+$, formed in the field-free region between the ion source and reflectron, were recorded at 14 decreasing reflector voltage intervals. The resulting 14 mass spectral segments were pasted in-line using the FAST algorithm provided by Bruker. Mass calibration at each PSD spectral segment was performed automatically by Bruker's spectral pasting algorithm using ACTH 18-39 as calibrant.

The ESI experiments were conducted with a Bruker Esquire-LC ion trap mass spectrometer (Billerica, MA). A syringe pump was used to nebulize at a rate of 5 μL/min, through a grounded needle, 25–50 μM solutions of the dendrimer in methanol–water (75:25) or benzene–acetic acid (≥85:≤15). The entrance of the sampling capillary, which is directed at a right angle to the spraying needle, was set at −4000 V relative to the needle; the potential difference between the capillary exit and skimmer 1 was 130 V. Nitrogen served as both the nebulizing gas (15 psi) and drying gas (5 L/min, 300 °C). These parameters led to the formation of $[M + nH]^{n+}$ ions (n = 1–4) from DAB-*dendr*-$(NH_2)_{16}$. CAD spectra of the singly and doubly protonated dendrimer (n = 1 and 2) were obtained by isolating the corresponding monoisotopic precursor ions and exciting them to fragment with a radiofrequency (RF) that was resonant with their frequency of motion inside the trap [29]. The precursor ions are accelerated in this process and collide with the helium buffer gas in the ion trap, thereby producing fragments; the RF amplitudes (V_{p-p}) used ranged between 0.9 and 1.8 V and the activation time was 40 ms.

DAB-*dendr*-$(NH_2)_{16}$ (propylene imine hexadecaamine dendrimer generation 3.0) was purchased from Sigma and dithranol from ICN Biomedicals Inc. (Aurora, OH). HPLC-grade solvents and acetic acid were purchased from Sigma or Aldrich. All chemicals were used as received from the manufacturer.

3. Results

3.1. MALDI-PSD spectra of $[M + H]^+$ in polar protic vs. nonpolar solvents

Four different solvents were utilized to dissolve the dendrimer upon MALDI sample preparation. The selected solvents were chloroform, acetonitrile–ethanol–water mixture (50:45:5), methylene chloride and benzene. Table 1 lists the dipole moments and pK_α values of these molecules [30–32], which constitute pertinent measures of their polarity and acidity, respectively. Chloroform is the polar protic (good) and benzene the nonpolar (bad) solvent used in the NMR study of Rinaldi and co-workers [8]; as mentioned in the introduction, these authors found that DAB-*dendr*-$(NH_2)_{16}$ ("DAB-16") attains an extended chain conformation in $CHCl_3$ but a folded (or intertwined) conformation in C_6H_6. Two additional solvents, viz. an acetonitrile–ethanol–water (50:45:5) mixture and methylene chloride were also assessed in the present study. The former is similar to the methanol–water (75:25) mixture used in ESI experiments of DAB dendrimers [25–27]; we chose acetonitrile–ethanol–water instead because this combination gave rise to MALDI-PSD spectra with a substantially higher signal:noise ratio than either methanol, methanol–water (75:25), ethanol, or ethanol–water (75:25) solvents.

Table 1
Dipole moments and pK_α values of solvents used in MALDI sample preparation and/or for ESI

Solvent	Dipole moment[a] (Debye)	pK_α[b]
CH_3CO_2H	1.74	4.76
CH_3OH	1.70	15.00
H_2O	1.85	15.70
CH_3CH_2OH	1.69	16.00
CH_3CN	3.92	25.00
$CHCl_3$	1.01	25.00[c]
CH_2Cl_2	1.60	–[d]
C_6H_6	0.00	43.00

[a] [30].
[b] [31].
[c] [32].
[d] Unknown; should lie between 25 and 43.

PSD spectra of $[M + H]^+$ (*m*/*z* 1687) were acquired using each of the four solvents in the sample preparation procedure. The spectrum obtained with chloroform is displayed in Fig. 1. It contains abundant fragments at *m*/*z* 871, 400, 172 and 58, which also dominated the reported ESI-CAD spectra of protonated DAB-16 [26,27]. The majority of fragment ions in the PSD spectrum of Fig. 1 can be rationalized by intramolecular nucleophilic substitution reactions (S_N2-type), as shown in Scheme 2 [27]. In these dissociations, a C atom in α-position to the protonated amine (leaving group) is attacked by an adjacent amine group (nucleophile) to produce a quaternary ammonium ion plus a neutral amine. Depending on the protonation site and the location of the attacking nucleophile (cf. Scheme 2), several different S_N2 displacements are possible. Table 2 summarizes the fragments arising upon such competitive processes from $[M + H]^+$ of DAB-16, using the nomenclature proposed by McLuckey et al. [27]: G_n gives the generation of the protonated nitrogen (G_0, H^+ on a core N atom; G_1, H^+ on a first generation N atom; etc.); and A or B denote S_N2 reactions in which a carbon in α-position to the charge is attacked by an adjacent N atom in the interior (A) or exterior (B) of the dendrimer. Scheme 2 illustrates the reactions ensuing from precursor ions that are protonated at the most basic site, i.e., the DAB core (N of 0th generation).

The G_1(A) and G_2(A) products (*m*/*z* 1327 and 1556), which originate from $[M + H]^+$ ions carrying the proton at a tertiary nitrogen of the first and second generation, respectively, have markedly lower abundances than the G_0(A) product (*m*/*z* 871); this observation suggests that protonation mainly occurs at one of the core nitrogens, which exhibit the highest

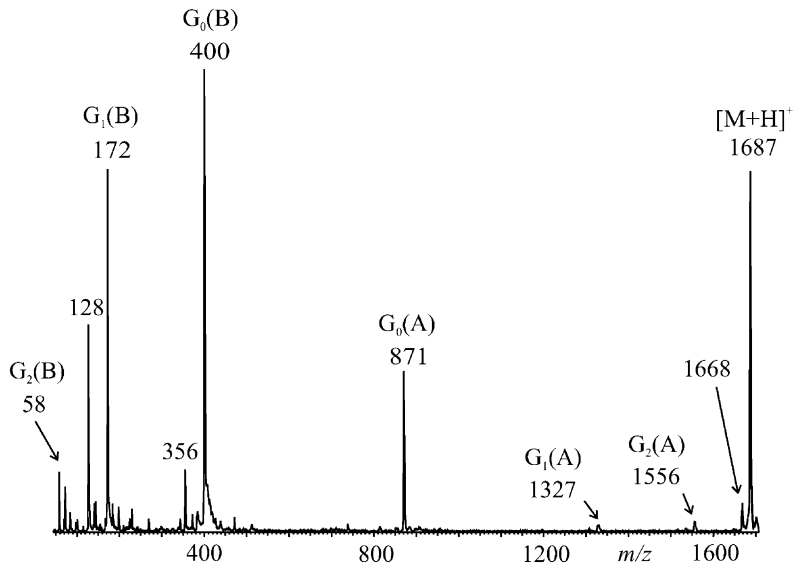

Fig. 1. MALDI-PSD spectrum of $[M + H]^+$ from DAB-*dendr*-$(NH_2)_{16}$, obtained from a sample dissolved in chloroform.

intrinsic basicity [26,27]. Similarly, G_0(B) gives rise to more intense fragments than either G_1(B) or G_2(B). Note, however, that the G_n(B) processes, involving attack of the charge site by an adjacent N nucleophile from the exterior, dominate in comparison to the G_n(A) processes. Two plausible explanations can be offered for this behavior: (a) G_n(B) generally have lower *m*/*z* values and could, thus, arise by sequential decomposition of the heavier G_n(A) fragments; (b) there are twice as many nucleophiles in exterior positions (for any given protonation site), which favors kinetically the formation of G_n(B).

The ions listed in Table 2 are virtually all fragments observed in ESI-CAD spectra of protonated DAB-16 (methanol–water solvent) [26,27]. They are also present in the MALDI-PSD spectrum of $[M+H]^+$ produced from a $CHCl_3$ solution (Fig. 1). The PSD spectrum contains additional fragments, mainly below *m*/*z* 871, most prominently at *m*/*z* 356 and 128. These are ascribed to consecutive dissociations of the major fragments; their enhanced yield upon MALDI-PSD vs. ESI-CAD points out that MALDI creates $[M + H]^+$ ions with a higher degree of internal excitation than ESI (vide infra).

Table 2
Fragments from $[M + H]^+$ of DAB-*dendr*-$(NH_2)_{16}$ (*m*/*z* 1686.7) generated via intramolecular S_N2 reactions

S_N2 process	*m*/*z* of quaternary ammonium ion	Mass of neutral amine (u)	Structure of fragment ion or neutral loss; R = $CH_2CH_2CH_2N$
G_2(A)	1555.5	131.2	Loss of $HN(RH_2)_2$
G_1(A)	1327.3	359.4	Loss of $HN[R(RH_2)_2]_2$
G_0(A)	870.8	815.9	Loss of $HN\{R[R(RH_2)_2]_2\}_2$[a]
G_0(B)	400.4	1286.3	Cyclo-$CH_2CH_2CH_2N^+[R(RH_2)_2]_2$[a]
G_1(B)	172.2	1514.5	Cyclo-$CH_2CH_2CH_2N^+(RH_2)_2$
G_2(B)	58.0	1628.7	Cyclo-$CH_2CH_2CH_2N^+H_2$[b]

[a] Structures shown in Scheme 2.
[b] Azetidinium cation.

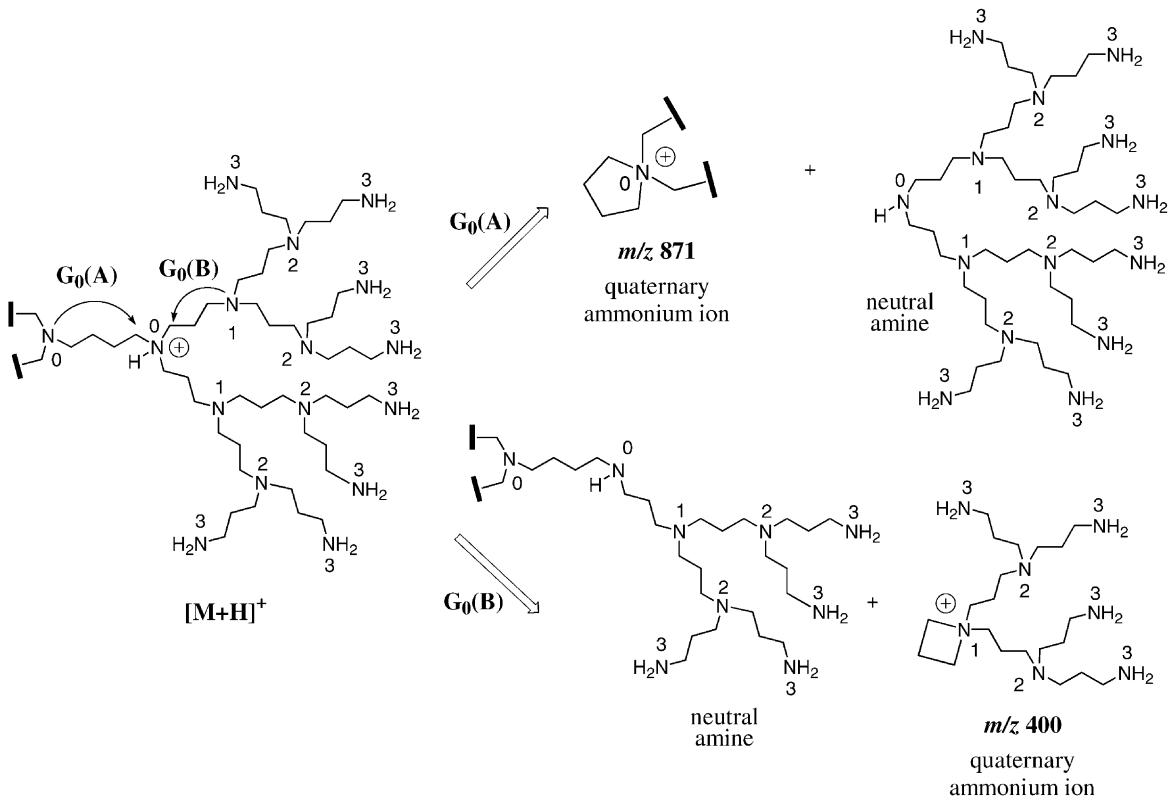

Scheme 2. Intramolecular nucleophilic substitution (S_N2) reactions leading to the formation of *m/z* 400 and 871 from $[M+H]^+$ of DAB-16. Only the DAB core and one half of the dendrimer are shown. The numbers next to the N atoms indicate their generation.

Our MALDI-PSD spectra obtained using the other three solvents show considerable and reproducible differences only in the region *m/z* 800–1687 which, therefore, is presented here in detail. Most pronounced are the differences between the PSD spectra resulting from the dendrimer dissolved in chloroform (polar protic) vs. the dendrimer dissolved in benzene (nonpolar); these spectra are contrasted in Fig. 2. The spectrum acquired with $CHCl_3$, Fig. 2(a), contains G_1(A) and G_2(A) products, as well as a sizable fragment at *m/z* 1668 corresponding to a loss of 19 u. The latter product is attributed to the elimination of NH_3 and H_2, proceeding from $[M+H]^+$ ions that are protonated at the primary amine sites (Scheme 3). Initially, a cyclic secondary ammonium ion is formed via S_N2 displacement of ammonia by a neighboring primary amine group. Consecutively, H_2 elimination, a well documented reaction of primary and secondary ammonium ions [33] takes place to give the observed product at *m/z* 1668, an immonium cation. The absence of a measurable *m/z* 1670 suggests that the MALDI-generated $[M+H]^+$ ions probed upon PSD have sufficient internal energies to lose both NH_3 and H_2. In the PSD spectrum of $[M+H]^+$ desorbed from a C_6H_6 solution (Fig. 2(b)), processes G_1(A), *m/z* 1327, and G_2(A), *m/z* 1556, essentially disappear below noise level, and the extent of NH_3+H_2 loss, *m/z* 1668, decreases markedly. The implications of this result will be discussed after the description of ESI data (vide infra).

We could not find another nonpolar solvent, besides benzene, in which DAB-16 was sufficiently soluble to provide useable MALDI and MALDI-PSD mass spectra. On the other hand, two more polar solvents were used, namely CH_2Cl_2 (aprotic) and

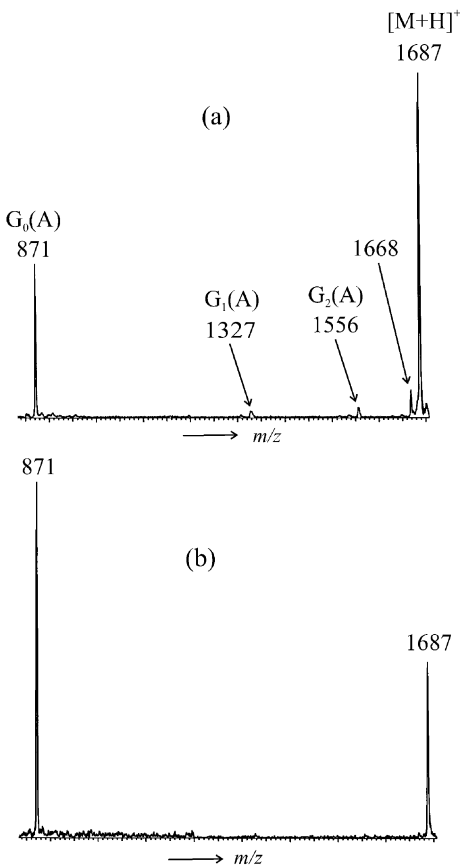

Fig. 2. Partial MALDI-PSD spectra (*m/z* 850–1700 region) of $[M + H]^+$ from DAB-*dendr*-$(NH_2)_{16}$, obtained from a sample dissolved in (a) chloroform and (b) benzene.

acetonitrile–ethanol–water mixture (protic). The latter solvent, which is quite analogous to the solvent used in previous ESI studies [25–27], gives comparable results to those observed with $CHCl_3$ (Table 3), albeit with a somewhat poorer signal-to-noise ratio. In contrast, CH_2Cl_2 leads to substantially reduced fragment ion abundances between *m/z* 871 and 1687, especially for G_1(A) (Table 3). CH_2Cl_2 and $CHCl_3$ have similar polarities (Table 1), but $CHCl_3$ also is acidic. It is evident, based on the trends of Table 3, that G_1(A), G_2(A) and $NH_3 + H_2$ loss progress most efficiently if the solvent used in MALDI sample preparation contains acidic protons.

3.2. ESI-CAD spectra of $[M + H]^+$ in polar protic vs. nonpolar solvents

Since the MALDI-PSD spectra of $[M+H]^+$ depend on the solvent used in sample preparation, the solvent could also play a role in the fragmentations occurring from ESI-generated $[M + H]^+$. This hypothesis was tested by acquiring CAD spectra of $[M+H]^+$ sprayed from a polar protic vs. a nonpolar solvent. Again, we focused on the region *m/z* 871–1687, in which the fragment ion abundances appear to be most sensitive to the nature of the solvent.

A 75:25 mixture of methanol water was selected as the polar solvent representative; this was the solvent of choice in the previous ESI studies of DAB dendrimers [25–27]. (Chloroform could not be used because it degrades PEEK materials in the spray chamber of the instrument.) Benzene was chosen as the nonpolar solvent representative; a modifier had to be added, in this case, to aid in protonation of the sample, because benzene cannot accomplish the task by itself. The modifier was acetic acid. Various experiments were run to find the optimal concentration of acetic acid, such that $[M + H]^+$ is formed with sufficient yield for MS/MS

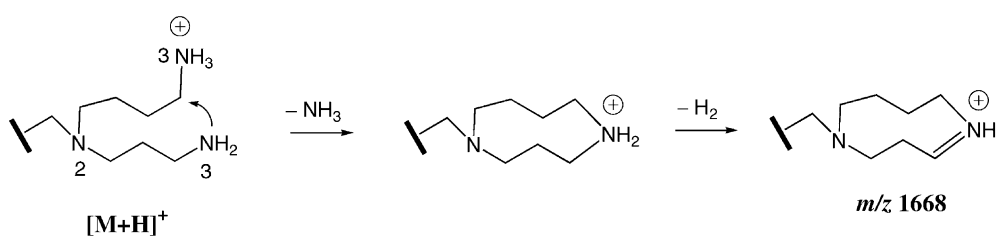

Scheme 3. Formation of *m/z* 1668 fragment from protonated DAB-16 via consecutive NH_3 and H_2 losses.

Table 3
MALDI-PSD fragments (*m/z* 870–1687 region) from $[M + H]^+$ of DAB-*dendr*-$(NH_2)_{16}$, desorbed from samples prepared in four different solvents[a]

Solvent	*m/z*			
	871, G_0(A)	1327, G_1(A)	1556, G_2(A)	1668, $-(NH_3 + H_2)$
$CHCl_3$	100	4.3	6.7	17
$CH_3CN/C_2H_5OH/H_2O$	100	4.6	6.4	7.8
CH_2Cl_2	100	<0.6[b]	1.8	4.2
C_6H_6	100	<0.6[b]	<0.6[b]	1.3

[a] Peak intensity relative to *m/z* 871 (±40%).
[b] In noise level.

but with the least possible amount of acetic acid, so that the solvent remains significantly less protic than methanol–water. A 5–15% (v/v) solution of acetic acid in benzene accomplished this purpose.

The CAD spectrum of $[M+H]^+$ from DAB-16 dissolved in methanol–water (75:25) is depicted in Fig. 3. It contains peaks at *m/z* 871, 1327 and 1556, originating from processes G_n(A), $n = 0$–2, in good agreement with the MALDI-PSD spectrum measured using $CHCl_3$ (Fig. 2(a)). In addition, the loss of NH_3 takes place (*m/z* 1670). The ammonia loss is not accompanied by consecutive elimination of H_2, as was observed in the case of MALDI-PSD. This difference is presumably due to the higher internal energy content of $[M+H]^+$ precursor ions in MALDI vs. ESI experiments (vide supra). Further, the relative abundance of NH_3 loss is found to vary significantly in replicable measurements. The trajectory of this fragment ion (*m/z* 1670) in the trap could be influenced by the resonance excitation applied to $[M + H]^+$ (*m/z* 1687) due to the similarity in mass of these two cations; the product of NH_3 loss is, therefore, not used in the evaluation of solvent, concentration or collision energy effects.

A minimum of 0.9 V resonance excitation amplitude (V_{p-p}) is necessary to induce CAD at the activation time used. When V_{p-p} is increased to 1.2 V (+33%), the intensity of $[M + H]^+$ decreases dramatically relative to that of the major G_0(A) product (Table 4), owing to an enhanced dissociation efficiency and probably also partial resonance excitation ejection.

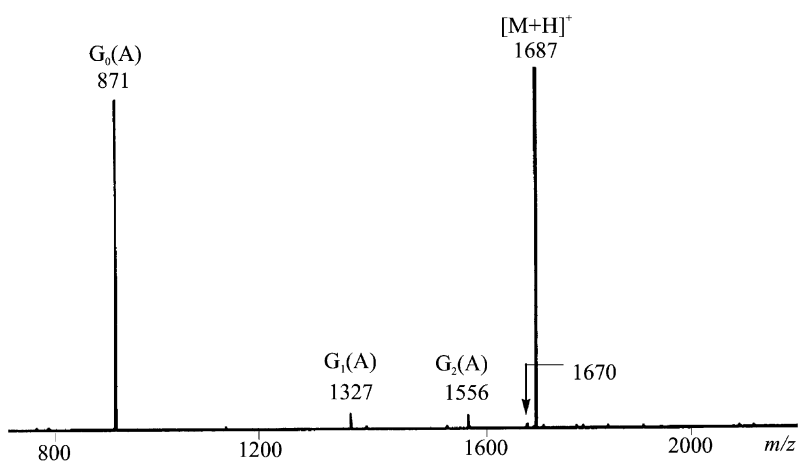

Fig. 3. Partial ESI-CAD spectrum (*m/z* 800–2000 region) of $[M + H]^+$ from DAB-*dendr*-$(NH_2)_{16}$, obtained from a sample dissolved in methanol–water (75:25). The RF amplitude (V_{p-p}) was 0.9 V.

Table 4
ESI-CAD fragments (*m/z* 871–1687 region) from $[M + H]^+$ of DAB-*dendr*-$(NH_2)_{16}$, sprayed from different solutions[a]

Solvent	Concentration (μM)	V_{p-p} (V)	*m/z*			
			871, $G_0(A)$	1327, $G_1(A)$	1556, $G_0(A)$	1687, $[M + H]^+$
CH_3OH/H_2O	50	0.9	100	4.3	4.3	651
	50	1.2	100	4.3	4.1	23
	25	1.2	100	3.9	3.8	14
C_6H_6/5% acetic acid	50	0.9	100	3.2	2.6	2233
	50	1.2[b]	100	5.7	4.0	0.7
C_6H_6/15% acetic acid	50	0.9	100	2.7	2.2	547
	50	1.2	100	5.0	6.0	63

[a] Peak intensity relative to *m/z* 871 (±15%).
[b] No measurable change in relative fragment ion abundances at 1.6 V.

At the same time, the relative intensities of $G_0(A)$, $G_1(A)$ and $G_2(A)$ at *m/z* 871, 1327 and 1556, respectively, do not change outside experimental error. Reducing the concentration of the dendrimer from 50 to 25 μM has also no effect on the relative abundances of *m/z* 871, 1327 and 1556 (Table 4).

With benzene as the ESI solvent, the dendrimer solution must be acidified to yield enough $[M + H]^+$ ions for a detectable CAD spectrum; we used ≥5% (v/v) acetic acid for this purpose. At the lowest possible collision energy, corresponding to $V_{p-p} = 0.9$ V, both *m/z* 1327 and 1556 are generated (Table 4). This is at odds with our MALDI-PSD spectra, where these fragments are not observed (<1% relative to *m/z* 871). Nonetheless, the polar protic dendrimer solution gives rise to much more $G_1(A)$ and $G_2(A)$ fragments relative to $G_0(A)$ fragment (cf. 0.9 V entries in Table 4), in agreement with the MALDI-PSD result.

Raising the acetic acid concentration to 15% increases the sensitivity but does not affect the relative abundances of *m/z* 871, 1327 and 1556 within experimental error limits (Table 4). Interestingly, the decrease in $[M + H]^+$ intensity with collision energy depends on acetic acid concentration. Also, in contrast to the $[M + H]^+$ precursor ions probed from methanol–water, the C_6H_6-sprayed $[M + H]^+$ ions form more *m/z* 1327 and 1556 upon increase of the collision energy (Table 4). The reason(s) for the last two phenomena is (are) difficult to discern. Overall, the ESI-CAD data from a protic vs. a nonpolar solvent are not as distinct as the respective MALDI-PSD data (perhaps because the addition of acetic acid to C_6H_6 creates a somewhat polar environment). Further, only under the mildest collisional activation conditions, PSD and CAD datasets follow the same trend, viz. a lower yield of $G_1(A)$ and $G_2(A)$ fragments, relative to $G_0(A)$, when the dendrimer ions are produced from the nonpolar (aprotic) solvent.

3.3. ESI-CAD spectra of $[M + 2H]^{2+}$ in polar protic vs. nonpolar solvents

ESI of DAB-16 coproduces multiply protonated precursor ions (see Section 2). In previous work, doubly and more highly charged precursor ions of DAB dendrimers were shown to fragment mainly by processes involving Coulomb repulsions and directed by protonation closer to the periphery of the dendrimer [25–27]. These earlier studies were performed exclusively in a polar protic solvent (75:25 methanol–water). Here, we investigate the role of ESI solvent on the fragmentation behavior of doubly protonated DAB-*dendr*-$(NH_2)_{16}$ (*m/z* 843.8).

When multiply charged dendrimers dissociate, both dissociation products can carry a charge and, hence, the amine product from the S_N2 process (see Scheme 2) can appear as a fragment ion (protonated amine) in the CAD spectrum [27]. The masses of the neutral amine fragments generated from DAB-16 are listed in Table 2; their protonated forms are termed

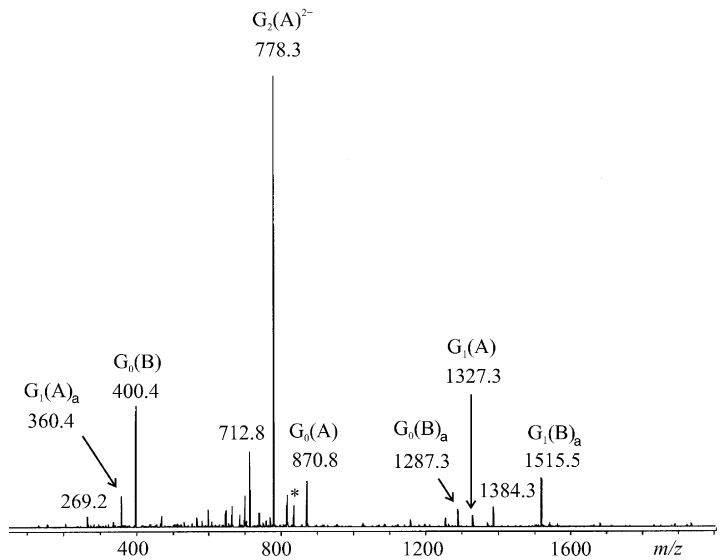

Fig. 4. ESI-CAD spectrum of $[M + 2H]^{2+}$ from DAB-*dendr*-$(NH_2)_{16}$, obtained from a sample dissolved in methanol–water (75:25). The RF amplitude (V_{p-p}) was 1.2 V and the low-mass cutoff at *m/z* 200. The asterisk indicates the location of $[M + 2H]^{2+}$ (*m/z* 843.8).

$G_n(A)_a$ or $G_n(B)_a$ (i.e., with a subscripted a) to distinguish them from the complementary quaternary ammonium ions formed during S_N2 reactions (note that the nominal masses of $G_n(A)_a$ or $G_n(B)_a$ are one mass unit higher than those of the respective neutral amines due to the added proton).

The CAD spectrum of $[M + 2H]^{2+}$ from the methanol–water solution is shown in Fig. 4 and agrees well with that reported by McLuckey et al. [27]. The major fragment at *m/z* 778.3 corresponds to a protonated *m/z* 1556 ion ($G_2(A)$ with two protons), arising by loss of the $HN(CH_2CH_2CH_2NH_2)_2$ wedge (131 u, cf. Table 2). The identified dissociation products are labeled on Fig. 4 and summarized in Scheme 4. It is noteworthy that processes G_0 are less efficient from $[M + 2H]^{2+}$ than $[M + H]^+$. The dication dissociates extensively by G_1- and G_2-type reactions, which are initiated by protonation away from the dendrimer core (Scheme 2), releasing outer dendrimer branches. In contrast, the cleavages of outer dendrimer wedges is much less pronounced in $[M + H]^+$, as is evident from the low extent in its spectra of processes $G_1(A)$ (loss of 359 u amine) and $G_2(A)$ (loss of 131 u amine).

Changing the solvent to benzene (plus 10% acetic acid) yields a CAD spectrum that is practically indistinguishable from that obtained using methanol–water (within the ±20% uncertainty of fragment ion

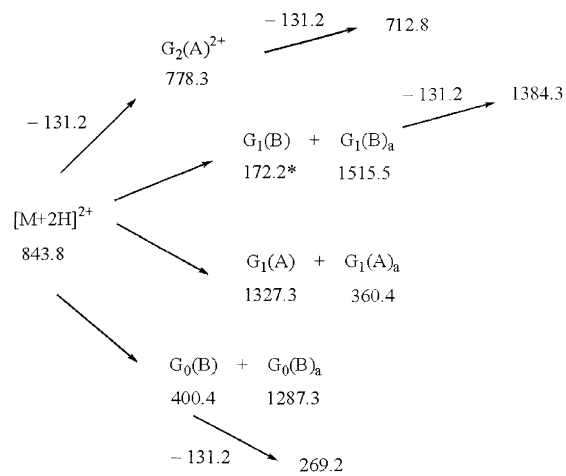

Scheme 4. Major CAD fragments from ESI-generated $[M+2H]^{2+}$ of DAB-16. The numbers give *m/z* values of ions or (those above or below the arrows) masses of neutral losses. Ion with asterisk next to its *m/z* value not observed in Fig. 4, because it lies outside the scan range (automatically set by software).

abundances in $[M+2H]^{2+}$ CAD spectra). We also find no measurable effect on the CAD fragmentation pattern of $[M+2H]^{2+}$ upon varying the resonance excitation amplitude between 1 and 2 V. These trends differ from those observed with $[M+H]^{+}$ and imply that the dication exists in only one conformation (vide infra).

4. Discussion

4.1. $[M + H]^{+}$ ions of DAB-dendr-$(NH_2)_{16}$

The fragmentation patterns of $[M+H]^{+}$ from protic vs. nonpolar solutions can be accounted for if different conformations are present in the two types of solvents, as indicated by NMR [8] and if these different conformations are preserved in the gaseous $[M+H]^{+}$ ions formed in the mass spectrometer.

Based on the MALDI-PSD experiments, cleavage of the second and first generation dendritic wedges (*m*/*z* 1556 and 1327, respectively) takes place if a polar protic solvent is used to dissolve DAB-16 upon sample preparation, but does not occur if a nonpolar solvent is employed for the latter purpose. In qualitative agreement with this result, the collision-induced dissociation of second and first generation branches from $[M + H]^{+}$ ions electrosprayed in a polar protic solution proceeds with a higher yield than from $[M + H]^{+}$ ions electrosprayed in a nonpolar solvent (at mild activation conditions).

The DAB molecule is polar and basic. A polar protic solvent can readily enter the interior cavities to form hydrogen bonds with the tertiary amines. This solvation stabilizes an extended conformation of DAB-16, in which the number of stabilizing intermolecular H bonds between solvent and dendrimer are maximized. On the other hand, a nonpolar solvent is less likely to penetrate the DAB dendrimer interior. Stabilizing H bonds can still be formed, now intramolecularly, if the periphery branches fold inside, so that the amine H atoms can interact with interior tertiary nitrogens (Scheme 5).

The solution conformations are "locked-in" when the solvent evaporates and the dendrimer crystallizes in the MALDI matrix upon sample preparation. Our MALDI-PSD data provide evidence that such conformational differences are maintained when the dendrimer molecules are desorbed as gaseous $[M + H]^{+}$ ions. After protonation, extended H bond networks are possible in folded conformations, particularly with charge sites away from the core (first and second generation), which are in closer proximity to adjacent basic sites (Scheme 6). This extra stability is a plausible rationale for the absence (or decreased yield) of losses from the outer branches (i.e. processes G_1(A)

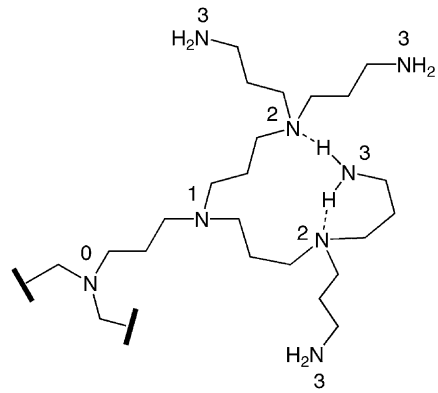

Scheme 5. Folding of outer DAB dendrimer chains to form intramolecular hydrogen bonds. The numbers next to the N atoms denote their generation.

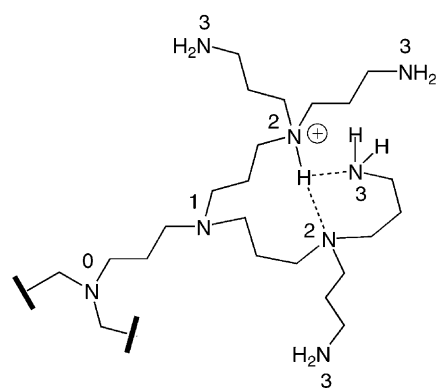

Scheme 6. Folding of protonated outer DAB dendrimer chains to form intramolecular hydrogen bonds. The numbers next to the N atoms denote their generation.

at *m*/*z* 1327 and G_2(A) at *m*/*z* 1556), when a nonpolar solvent is used.

In the ESI experiments, the addition of acetic acid to benzene appears to compromise the nonpolar environment, leading to less distinctive dissociation characteristics between methanol–water and benzene solutions. The discriminated dissociations (G_1(A) and G_2(A)) recover easily when the collision energy upon CAD is increased (Table 4) further suggesting that the degree of intramolecular H bonding is low in benzene doped with acetic acid.

It is conceivable that DAB-16 is protonated in the gas phase upon MALDI but in solution upon ESI (in the charged droplets). SANS experiments found that DAB conformations become more stretched after protonation [23]. This in turn provides an alternative explanation for the smaller solvent effect observed for ESI- vis à vis MALDI-generated $[M + H]^+$.

4.2. $[M + 2H]^{2+}$ ions of DAB-dendr-$(NH_2)_{16}$

The Coulomb repulsion between the two charges is minimized in stretched conformations, with the protons near higher generation N atoms. The considerable yield of G_1(A) and G_2(A) products with either solvent agrees well with such an extended conformation in both cases. Evidently, relief from Coulomb repulsion outweighs any stabilization brought upon by H bonding, and any folding present in M or $[M + H]^+$ cannot be maintained upon double protonation.

5. Conclusions

The MS/MS spectra of DAB-16 dendrimer ions, generated by MALDI or ESI, are found to depend on the solvent used to dissolve the dendrimer in the ionization procedure. Significant differences are observed between the MS/MS spectra resulting from MALDI of $CHCl_3$ (polar protic) and C_6H_6 (nonpolar) solutions. Elimination of the outer branches from $[M+H]^+$, i.e., of $HN(CH_2CH_2CH_2NH_2)_2$ (*m*/*z* 1556) and $HN[CH_2CH_2N(CH_2CH_2CH_2)_2]_2$ (*m*/*z* 1327), does not take place when $[M + H]^+$ is formed from a C_6H_6 solution. This result is attributed to a folded conformation, in which the periphery branches fold into the interior to enable hydrogen bonding between the primary external and tertiary internal amines; due to such intramolecular self-solvation, certain C–N bonds in $[M + H]^+$ cannot be efficiently cleaved. On the other hand, the polar solvent promotes formation of $[M + H]^+$ with an extended, unfolded conformation, from which outer branches can be cleaved. The same conformational differences were detected in solution by NMR [8]. The analogous trends of NMR (i.e., solution) and MS/MS (i.e., gas phase) data agree well with preservation in the gaseous $[M+H]^+$ ions of the dendrimer structure prevalent in solution.

In the ESI experiments, the nonpolar solvent must be acidified to yield the $[M + H]^+$ intensities needed for MS/MS. This in turn compromises the nonpolar character of the solvent, leading to smaller differences between MS/MS spectra acquired using a nonpolar (C_6H_6 doped with acetic acid) vs. a polar protic (methanol–water) solvent. The more striking differences of MALDI-MS/MS than ESI-MS/MS spectra in nonpolar vs. polar protic solvents may also reflect different places of $[M + H]^+$ formation, i.e., protonation in the gas phase in MALDI vs. protonation in solution in ESI. The latter process has been shown to stretch folded neutral dendrimers [23] and, hence, would diminish the extent of folding of the dendrimer in a nonpolar solvent.

It is noteworthy, that the $[M + 2H]^{2+}$ cations produced by ESI give the same MS/MS spectra irrespective of the solvent used in the ion generation step. The loss of outer branches always takes place (abundantly), consistent with an extended conformation, also for the nonpolar solvent. Thus, any conformational differences in the neutral or singly protonated dendrimer disappear after addition of another proton. This result reveals that minimization of like charge repulsions (best feasible in an extended conformation) increases the intrinsic stability (lowers the energy) more than conservation of intramolecular hydrogen bonds.

Acknowledgements

We thank the National Science Foundation (DMR-9703946), the Ohio Board of Regents—Hayes Investment Fund and the University of Akron for generous financial support. We are grateful to Dr. Michael J. Polce, Mark A. Arnould and Kathleen M. Wollyung for experimental assistance and helpful discussions and suggestions.

References

[1] A.W. Bosnan, H.M. Janssen, E.W. Meijer, Chem. Rev. 99 (1999) 1665.
[2] C.J. Hawker, J.M.J. Frechet, J. Am. Chem. Soc. 112 (1990) 7638.
[3] C.J. Hawker, J.M.J. Frechet, J. Chem. Soc. Chem. Commun. (1990) 1010.
[4] C. Wörner, R. Mülhaupt, Angew. Chem. Int. Ed. Engl. 32 (1993) 1306.
[5] E.M.M. De Brabander-van den Berg, E.W. Meijer, Angew. Chem. Int. Ed. Engl. 32 (1993) 1308.
[6] M. Chai, Y. Niu, W.J. Youngs, P.L. Rinaldi, Macromolecules 33 (2000) 5395.
[7] H. Kao, A.D. Stefanescu, K.L. Wooley, J. Schaefer, Macromolecules 33 (2000) 6214.
[8] M. Chai, Y. Niu, W.J. Youngs, P.L. Rinaldi, J. Am. Chem. Soc. 123 (2001) 4670.
[9] L. Balogh, D.R. Swanson, R. Spindler, D.A. Tomalia, Polym. Mater. Sci. Eng. 77 (1997) 118.
[10] N.B. Tan, Macromolecules 33 (2000) 4445.
[11] C.M. Whitehouse, R.N. Dreuer, M. Yamashita, J.B. Fenn, Anal. Chem. 57 (1985) 675.
[12] F. Hillenkamp, M. Karas, R.C. Beavis, B.T. Chait, Anal. Chem. 63 (1991) 1193A.
[13] J.C. Hummelen, J.L.J. van Dongen, E.W. Meijer, Chem. Eur. J. 3 (1997) 1489.
[14] L. Mingjun, J.M.J. Frechet, Polym. Bull. 43 (1999) 379.
[15] P.G. de Gennes, H. Hervet, J. Phys. Lett. Paris 44 (1983) L351.
[16] R.L. Lescanec, M. Muthukumar, Macromolecules 23 (1990) 2280.
[17] M.L. Mansfield, L.I. Klushin, Macromolecules 26 (1993) 4262.
[18] D. Boris, M. Rubenstein, Macromolecules 29 (1996) 7251.
[19] (a) R. Scherrenberg, B. Coussens, P. van Vliet, G. Edouard, J. Brackman, E. de Brabander, K. Mortensen, Macromolecules 31 (1998) 456;
(b) A. Sariban, J. Brickman, J. van Ruiten, R.J. Meier, Macromolecules 25 (1992) 5950.
[20] M. Murat, G.S. Grest, Macromolecules 29 (1999) 1278.
[21] P. Welch, M. Muthukumar, Macromolecules 31 (1998) 5892.
[22] S. De Backer, Y. Prinzie, W. Verheijen, M. Smet, K. Desmedt, W. Dehaen, F.C. De Schryver, J. Phys. Chem. A 102 (1998) 5451.
[23] A. Ramzi, R. Scherrenberg, J. Brackman, J. Joosten, K. Mortenson, Macromolecules 31 (1998) 1621.
[24] K.L. Busch, G.L. Glish, S.A. McLuckey, Mass Spectrometry/Mass Spectrometry: Techniques and Applications of Tandem Mass Spectrometry, VCH Publishers, New York, 1988.
[25] J.-W. Weener, J.L.J. van Dongen, E.W. Meijer, J. Am. Chem. Soc. 122 (1999) 10346.
[26] J. de Maaijer-Gielbert, C. Gu, Á. Somogyi, V.H. Wysocki, P.G. Kistemaker, T.L. Weeding, J. Am. Soc. Mass Spectrom. 10 (1999) 414.
[27] S.A. McLuckey, K.G. Asano, G. Schaaff, J.L. Stephenson Jr., Int. J. Mass Spectrom. 195/196 (2000) 419.
[28] B. Spengler, J. Mass Spectrom. 32 (1997) 1019.
[29] S.A. McLuckey, G.J. Van Berkel, D.E. Goeringer, G.L. Glish, Anal. Chem. 66 (1994) 689A.
[30] D.R. Lide (Ed.), Handbook of Chemistry and Physics, 71st Edition, CRC Press, Boca Raton, FL, 1990.
[31] T.H. Lowry, K.S. Richardson, Mechanism and Theory in Organic Chemistry, 3rd Edition, Harper & Row, New York, 1987.
[32] S.N. Ege, R.W. Kleinman, M.L.C. Carter, Study Guide for Organic Chemistry, 2nd Edition, Heath, Leungton, MA, 1989.
[33] R.D. Bowen, Mass Spectrom. Rev. 10 (1991) 225.